

with the SOMO in this direction. They would, however, be expected to have axial and not orthorhombic symmetry. A loosely bound complex with an interaction of the Ga atom with one double bond of the benzene ring, analogous to Kasai's description of $\text{Al}[\text{C}_6\text{H}_6]$, cannot be ruled out by this latter constraint. Furthermore, the possible necessity for the inclusion of quadrupole terms in the spin Hamiltonian could indicate a complex of lower symmetry.

Comparison of the unpaired spin populations of Ga atoms in benzene with those of Ga atoms in KCl, where $\rho_{4s} = 0.02$ and $\rho_{4p} = 0.7$,²⁵ indicates a lower unpaired 4p-spin population and a positive unpaired 4s-spin population in the ionic matrix.

The spectrum of Ga atoms in benzene is not saturated by high levels of microwave power, suggesting an efficient spin-lattice relaxation process, unlike group 1 metal atoms in hydrocarbon

matrices which are readily power saturated.

Finally, the formation of cyclohexadienyl in the Ga-benzene system suggests the intermediacy of the hydrogen atom that is not formed from the reactant benzene or the matrix adamantane. Reaction of Ga atoms with adventitious water is therefore the most likely source of H^\bullet . It may be relevant that we have not detected HGaoH under our experimental conditions, whereas HAlOH is often detected from Al atom reactions with, for example, allene while Al and benzene do not give $\text{C}_6\text{H}_7^\bullet$ in adamantane or upon warmup.

Acknowledgment. H.A.J. thanks NSERC for a postdoctoral fellowship, and J.A.H. and B.M. thank NATO for a collaborative research grant (442/82). We are grateful to Drs. J. R. Morton and K. F. Preston for many helpful discussions.

²⁹Si MAS NMR Investigation of the $\text{Na}_2\text{O}-\text{Al}_2\text{O}_3-\text{SiO}_2$ Glasses

Hideki Maekawa, Takashi Maekawa,[†] Katsuyuki Kawamura, and Toshio Yokokawa*

Department of Chemistry, Faculty of Science, Hokkaido University, Sapporo, 060 Japan

(Received: January 22, 1991)

²⁹Si nuclear magnetic resonance (MAS NMR) on sodium aluminosilicate glasses with composition range of $[\text{Na}]/[\text{Al}] \geq 1$ were investigated. Line shapes and chemical shifts suggested that numbers of nonbridging oxygen atoms increase linearly with $([\text{Na}] - [\text{Al}])/[\text{Si}]$, in agreement with the classical structural model. An addition of alumina into sodium silicate glasses caused ²⁹Si chemical shift to lower field (less shielded) and increment of line width of Q_n peaks with higher n value, where Q_n represents the SiO_4 tetrahedron with n bridging oxygen atoms connected to adjacent Si atom. It was suggested that aluminum atom tends to be coordinated with SiO_4 tetrahedra of most polymerized states. The reaction between Q_n structure units, $2Q_n = Q_{n-1} + Q_{n+1}$, seemed to proceed to the left direction with increasing aluminum oxide contents as NaAlO_2 into the sodium silicate glass.

Introduction

The atomic arrangements of aluminosilicates have been studied extensively because they are found in important rock-forming minerals and their melts are thought to be a general model for acidic magmas. It is also interesting that addition of aluminum into silicate glasses causes their glass forming tendency. Densities, viscosities, refractive indexes, thermal expansivities, etc., show drastic changes near the composition of atom ratio $[\text{Na}]/[\text{Al}] = 1$ ¹⁻⁶ and are thought to be accompanied by the change of coordination numbers of aluminum from four to six oxygen atoms. Thus, Galant¹ measured refractive indexes of sodium aluminosilicate glasses and proposed a structural model that, in the composition range $[\text{Na}]/[\text{Al}] > 1$, all Al^{3+} form AlO_4 tetrahedra accompanied by Na^+ ion as the charge compensator. The remaining sodium oxide modifies the silicate network ($\text{Si}-\text{O}-\text{Si}$) and creates nonbridging oxygen atoms (NBOs, $\text{Si}-\text{O}-\text{Na}^+$) bonded to only one silicon atom. While the observed physical properties suggest the validity of this structural model, spectroscopic observations have not always supported it. Bruckner et al.⁷ and Smets and Lommen⁸ concluded from $\text{O}(1s)$ XPS spectra that number of NBO goes zero even at the composition $[\text{Na}]/[\text{Al}] \approx 0.7$ and some AlO_6^{3-} might exist at the region of $[\text{Na}]/[\text{Al}] = 1$. On the other hand, Taskere et al.⁹ showed that number of NBO linearly changed with $([\text{Na}] - [\text{Al}])/[\text{Si}]$ and goes zero at $[\text{Na}]/[\text{Al}] = 1$, thus supporting the model. Other methods such as XRD,¹⁰ EXAFS,¹¹ Raman spectroscopy,¹² and MAS NMR¹³⁻¹⁸ were also employed, and wide varieties of the structural informations had been reported. Among them, ²⁹Si, ²⁷Al, and ²³Na MAS NMR with compositions at around $[\text{M}]/[\text{Al}] = 1$ ($\text{M} = \text{Li}, \text{Na}, \text{K}, 0.5\text{Ca}$) revealed the coordination number of aluminum to be four and Lowenstein's rule¹⁹ was obeyed. The chemical shifts

TABLE I: ²⁹Si Chemical Shift for Series 1 Glasses

syst	composition	chem shift
$\text{Na}_2\text{O}-\text{SiO}_2$	$1\text{Na}_2\text{O}-3\text{SiO}_2$	-94.8
	$1\text{Na}_2\text{O}-2\text{SiO}_2$	-87.7
	$2\text{Na}_2\text{O}-3\text{SiO}_2$	-83.5
	$1\text{Na}_2\text{O}-1\text{SiO}_2$	-75.1
1a, $\text{Na}_2\text{O}:\text{SiO}_2 = 1:3$	$3\text{Na}_2\text{O}-1\text{Al}_2\text{O}_3-9\text{SiO}_2$	-92.0
	$20\text{Na}_2\text{O}-1\text{Al}_2\text{O}_3-40\text{SiO}_2$	-87.4
1b, $\text{Na}_2\text{O}:\text{SiO}_2 = 1:2$	$9\text{Na}_2\text{O}-2\text{Al}_2\text{O}_3-18\text{SiO}_2$	-85.8
	$4\text{Na}_2\text{O}-1\text{Al}_2\text{O}_3-8\text{SiO}_2$	-87.0
	$3\text{Na}_2\text{O}-1\text{Al}_2\text{O}_3-6\text{SiO}_2$	-87.8
	$2\text{Na}_2\text{O}-1\text{Al}_2\text{O}_3-4\text{SiO}_2$	-85.0
	$3\text{Na}_2\text{O}-2\text{Al}_2\text{O}_3-6\text{SiO}_2$	-84.7
	$11\text{Na}_2\text{O}-9\text{Al}_2\text{O}_3-22\text{SiO}_2$	-85.3
1c, $\text{Na}_2\text{O}:\text{SiO}_2 = 2:3$	$6\text{Na}_2\text{O}-1\text{Al}_2\text{O}_3-9\text{SiO}_2$	-81.2
	$4\text{Na}_2\text{O}-1\text{Al}_2\text{O}_3-6\text{SiO}_2$	-81.5
	$2\text{Na}_2\text{O}-1\text{Al}_2\text{O}_3-3\text{SiO}_2$	-80.9
	$9\text{Na}_2\text{O}-1\text{Al}_2\text{O}_3-9\text{SiO}_2$	-74.6
1d, $\text{Na}_2\text{O}:\text{SiO}_2 = 1:1$	$3\text{Na}_2\text{O}-1\text{Al}_2\text{O}_3-3\text{SiO}_2$	-75.0
	$5, \text{Na}_2\text{O}:\text{Al}_2\text{O}_3 = 1:1$	
	SiO_2	-110.9
	$1\text{Na}_2\text{O}-1\text{Al}_2\text{O}_3-6\text{SiO}_2$	-97.9
	$1\text{Na}_2\text{O}-1\text{Al}_2\text{O}_3-4\text{SiO}_2$	-92.8
	$1\text{Na}_2\text{O}-1\text{Al}_2\text{O}_3-2\text{SiO}_2$	-86.0

were also discussed in terms of T-O-T ($\text{T} = \text{Si}, \text{Al}$) bond angles. Nevertheless, detailed informations of SiO_4 or AlO_4 site distri-

(1) Galant, E. I. *The Structure of Glass* (translated from the Russian); Consultants Bureau: New York, 1960; Vol. 2, p 451. Proceedings of the Third All-Union Conference on the Glassy State, Leningrad, 1959.

(2) Day, D. E.; Rindone, G. E. *J. Am. Ceram. Soc.* **1962**, *45*, 489.

(3) Lacy, E. D. *Phys. Chem. Glasses* **1963**, *4*, 234.

(4) Shelby, J. E. *J. Appl. Phys.* **1979**, *49*, 5885.

(5) Riebling, E. F. *J. Chem. Phys.* **1966**, *44*, 2857.

(6) Klonkowski, A. *Phys. Chem. Glasses* **1983**, *24*, 166.

(7) Bruckner, R.; Chun, H.-U.; Goretzki, H.; Sammet, M. *J. Non-Cryst. Solids* **1980**, *42*, 49.

[†] Present address: Department of Resources Chemistry, Faculty of Engineering, Ehime University, Matsuyama, 790 Japan.

TABLE II: ²⁹Si MAS NMR Chemical Shift, Peak Intensity, Half-Width of Each Q_n Species and Calculated Numbers of Nonbridging Oxygens from Peak Intensity^a

<i>N</i> _{Al}		chem shift, ppm	intensity	half-width, ppm	NBO calc	<i>N</i> _{Al}		chem shift, ppm	intensity	half-width, ppm	NBO calc
(a) Series 2a											
0.0	Q ₂	-77.0	3	4.0	0.49	0.4	Q ₃	-90.7	52	5.7	0.52
	Q ₃	-92.2	47	5.6			Q ₄	-101.0	48	7.2	
	Q ₄	-105.6	50	6.5		0.5	Q ₃	-89.9	52	6.0	0.52
0.1	Q ₃	-92.2	50	5.5	0.50		Q ₄	-99.3	48	7.4	
	Q ₄	-105.0	50	6.5		1.0	Q ₃	-86.8	55	6.4	0.55
0.2	Q ₃	-92.2	52	5.5	0.52		Q ₄	-94.0	45	7.4	
	Q ₄	-104.1	48	6.5		1.5	Q ₃	-83.5	65	6.1	0.66
0.3	Q ₃	-91.0	53	5.7	0.53		Q ₄	-90.1	35	7.0	
	Q ₄	-102.4	47	7.2							
(b) Series 2b											
0.0	Q ₁	-67.2	3	3.0	1.47		Q ₃	-84.9	58	5.7	
	Q ₂	-76.6	42	3.4		0.4	Q ₁	-67.0	3	3.6	1.44
	Q ₃	-86.4	55	5.1			Q ₂	-76.0	38	3.6	
0.1	Q ₁	-67.0	4	3.6	1.47		Q ₃	-83.9	59	5.9	
	Q ₂	-76.5	41	3.5		0.5	Q ₁	-67.0	3	3.6	1.42
	Q ₃	-86.0	55	5.2			Q ₂	-75.8	36	3.8	
0.2	Q ₁	-67.0	2	3.6	1.48		Q ₃	-83.0	61	6.2	
	Q ₂	-76.5	43	3.6		1.0	Q ₂	-75.6	60	5.2	1.60
	Q ₃	-85.5	55	5.4			Q ₃	-82.6	40	6.0	
0.3	Q ₁	-67.0	2	3.0	1.43	1.5	Q ₂	-73.5	55	4.8	1.55
	Q ₂	-76.3	40	3.6			Q ₃	-80.1	45	5.2	
(c) Series 2c											
0.0	Q ₀	-59.5	3	3.0	2.48	0.3	Q ₀	-59.5	4	3.0	2.46
	Q ₁	-66.7	39	2.4			Q ₁	-66.5	36	2.4	
	Q ₂	-75.6	54	3.8			Q ₂	-74.6	56	4.5	
	(Q ₃)	-85.0	4	5.0			(Q ₃)	-84.5	4	5.0	
0.1	Q ₀	-59.5	3	3.0	2.48	0.4	Q ₀	-59.5	5	3.0	2.47
	Q ₁	-66.7	39	2.4			Q ₁	-66.3	36	2.5	
	Q ₂	-75.3	53	4.0			Q ₂	-74.0	56	4.6	
	(Q ₃)	-85.0	5	5.0			(Q ₃)	-84.5	3	5.0	
0.2	Q ₀	-59.5	3	3.0	2.49	0.5	Q ₀	-59.4	5	3.0	2.43
	Q ₁	-66.6	38	2.4			Q ₁	-66.1	34	2.5	
	Q ₂	-74.9	55	4.2			Q ₂	-73.5	59	4.8	
	(Q ₃)	-84.5	4	5.0			(Q ₃)	-84.5	2	5.0	
(d) Series 3											
0.0	(Q ₂)	-77.0	3	4.0	0.53		Q ₄	-104.0	69	7.5	
	Q ₃	-92.2	47	5.6		0.3	Q ₃	-91.8	20	5.7	0.20
	Q ₄	-105.6	50	6.5			Q ₄	-103.0	80	7.8	
0.1	(Q ₂)	-78.0	1	4.0	0.41	0.4	Q ₃	-91.2	10	5.7	0.10
	Q ₃	-92.5	39	5.4			Q ₄	-103.0	90	8.3	
	Q ₄	-105.0	60	7.0		0.5	Q ₃	-90.0	3	5.7	0.03
0.2	(Q ₂)	-78.0	1	4.0	0.32		Q ₄	-101.5	97	9.0	
	Q ₃	-92.3	30	5.7							
(e) Series 4											
<i>N</i> _{Al} = 0.0	Q ₁	-67.2	3	3.0	1.48	<i>N</i> _{Al} = 0.3	Q ₁	-68.0	1	3.0	1.19
<i>N</i> _{nbo} = 1.5	Q ₂	-76.6	42	3.4		<i>N</i> _{nbo} = 1.2	Q ₂	-76.9	20	3.4	
	Q ₃	-86.4	55	5.1			Q ₃	-86.3	76	5.4	
<i>N</i> _{Al} = 0.1	Q ₁	-67.8	1	3.0	1.33		Q ₄	-97.6	3	5.5	
<i>N</i> _{nbo} = 1.4	Q ₂	-76.8	33	3.4		<i>N</i> _{Al} = 0.4	Q ₂	-78.2	15	3.4	1.10
	Q ₃	-86.5	64	5.2		<i>N</i> _{nbo} = 1.1	Q ₃	-87.5	80	5.4	
	Q ₄	-97.2	2	5.5			Q ₄	-98.6	5	5.5	
<i>N</i> _{Al} = 0.2	Q ₁	-67.8	1	3.0	1.25	<i>N</i> _{Al} = 0.5	Q ₂	-77.8	10	3.5	1.03
<i>N</i> _{nbo} = 1.3	Q ₂	-76.8	26	3.4		<i>N</i> _{nbo} = 1.0	Q ₃	-87.2	83	5.5	
	Q ₃	-86.3	70	5.4			Q ₄	-97.4	7	5.5	
	Q ₄	-97.2	2	5.5							

^a *N*_{Al} represents 4[Al]/([Al] + [Si]).

bution have not been clarified. In the present work, we observed the compositional dependence of the ²⁹Si MAS NMR spectra of

sodium aluminosilicate glasses in a wider composition range. The role of aluminum in the silicate network structure will be discussed

- (8) Smets, B. M. J.; Lommen, T. P. A. *Phys. Chem. Glasses* **1981**, *22*, 158.
 (9) Taskere, G. W.; Uhlmann, D. R.; Onorato, P. I. K.; Alexander, M. N.; Struck, C. W. *J. Phys. (Paris)* **1985**, C8-273.
 (10) Taylor, M.; Brown Jr., G. E. *Geochim. Cosmochim. Acta* **1979**, *43*, 1467.
 (11) McKeown, D. A.; Waychunas, G. A.; Brown Jr., G. E. *J. Non-Cryst. Solids* **1985**, *74*, 349.
 (12) Domine, F.; Piriou, B. *Am. Mineral.* **1986**, *71*, 38.
 (13) Murdoch, J. B.; Stebbins, J. F.; Carmichael, I. S. E. *Am. Mineral.* **1985**, *70*, 332.

- (14) Kirkpatrick, R. J.; Oestrike, R.; Weiss Jr., C. A.; Smith, K. A.; Oldfield, E. *Am. Mineral.* **1986**, *71*, 705.
 (15) DeJong, B. H. W. S.; Schramm, C. M.; Parziale, V. E. *Geochim. Cosmochim. Acta* **1983**, *47*, 1223.
 (16) Lippmaa, E.; Samoson, A.; Magi, M. *J. Am. Chem. Soc.* **1986**, *108*, 1730.
 (17) Oestrike, R.; Yang, W.-H.; Kirkpatrick, J.; Hervig, R. L.; Navrotsky, A.; Montez, B. *Geochim. Cosmochim. Acta* **1987**, *51*, 2199.
 (18) Engelhardt, G.; Nofz, M.; Wihsmann, F. G.; Magi, M.; Samoson, A.; Lippmaa, E. *Phys. Chem. Glasses* **1985**, *26*, 157.

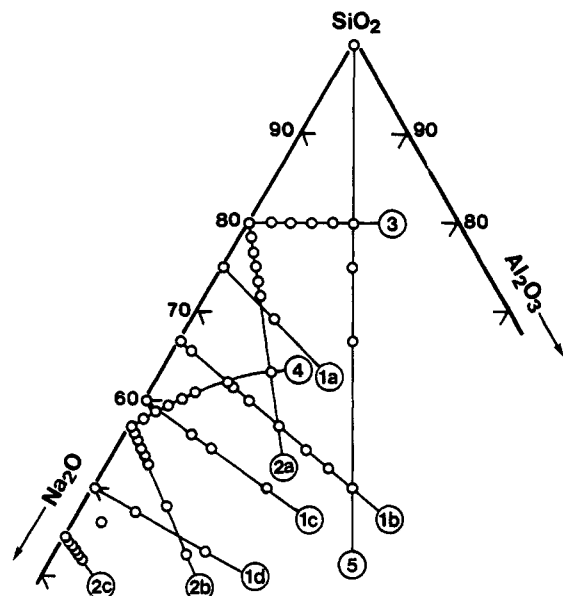


Figure 1. Five series of the glasses shown in the composition diagram for $\text{Na}_2\text{O}-\text{Al}_2\text{O}_3-\text{SiO}_2$ system.

based on the ^{29}Si NMR chemical shift analysis and peak separation.

Experimental Section

Samples were prepared from reagent grade Na_2CO_3 , Al_2O_3 , and SiO_2 . Mixed starting materials were carefully melted in Pt crucible at 1250–1400 °C for 3 h. Then the samples were quenched in water or liquid nitrogen. All samples were optically clear. The nominal compositions of the glasses are cited in Tables I and II and Figure 1. They are composed of five series in addition to the binary sodium silicates.²⁰ Series 1 (a–d) are the glasses with composition of constant $[\text{Na}]/[\text{Si}]$ ratios; in series 4, the composition is kept to maintain $N_{\text{nbo}} + N_{\text{Al}} = 1.5$ with the following definitions of N_{nbo} , N_{Al} , and N_{Al}' :

$$N_{\text{nbo}} = \frac{[\text{NBO}]}{[\text{Si}]} = ([\text{Na}] - [\text{Al}]) / [\text{Si}] \quad (1a)$$

$$N_{\text{Al}} = \frac{4[\text{Al}]}{[\text{Si}]} \frac{[\text{Si}]}{[\text{Al}] + [\text{Si}]} = \frac{4[\text{Al}]}{[\text{Al}] + [\text{Si}]} \quad (1b)$$

$$N_{\text{Al}}' = 4[\text{Al}] / [\text{Si}] \quad (1c)$$

Here N_{Al} is the number of Si–O–Al linkage per Si atom when Lowenstein's rule is disregarded. When the rule is obeyed, the N_{Al}' will be more appropriate instead of N_{Al} . The condition of $N_{\text{nbo}} + N_{\text{Al}} = 1.5$ means the total of Si–O– Na^+ and Si–O–Al linkages is kept constant.

2a, 2b, and 2c are systems of $\text{Na}_2\text{O} \cdot 4\text{SiO}_2 + \text{NaAlO}_2$, $3\text{Na}_2\text{O} \cdot 4\text{SiO}_2 + \text{NaAlO}_2$, and $5\text{Na}_2\text{O} \cdot 4\text{SiO}_2 + \text{NaAlO}_2$, respectively, where N_{Al} ranged from 0 to 1.5 with constant N_{nbo} value. Compositions of series 3 and 5 are $(1-x)\text{Na}_2\text{O} \cdot x\text{Al}_2\text{O}_3 \cdot 4\text{SiO}_2$ ($x = 0-0.5$) and $x\text{NaAlO}_2 \cdot (1-x)\text{SiO}_2$ ($x = 0-0.5$), respectively. As NaAlO_2 content increases in series 5, Si^{4+} ions in the network are replaced by Al^{3+} ions accompanied by Na^+ to compensate the charge difference. Each of the glass will be denoted such as 2a-1, 2a-2, 2a-3, etc.

We added 0.05–0.1 wt % Fe_2O_3 in some glasses (series 2–4) to reduce the relaxation time of ^{29}Si nuclei. No appreciable difference of the NMR spectra was found between glasses with and without Fe_2O_3 . Measurements of ^{29}Si MAS NMR were made with Bruker MSL-400 (for the samples of series 1 and 5 without addition of Fe_2O_3) and MSL-200 spectrometer (series 2–4) operated at 79.52 and 39.76 MHz for ^{29}Si , respectively. A pulse

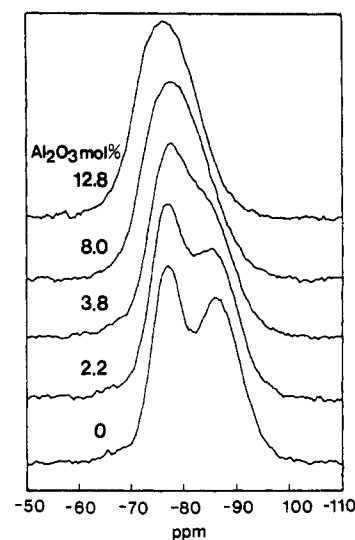


Figure 2. ^{29}Si MAS NMR spectra for series 2b glasses. Compositions are $3\text{Na}_2\text{O} \cdot 4\text{SiO}_2 + \text{NaAlO}_2$.

width of 3 μs (45° pulse) and dead time of 20 μs were used. A sweep width of 30 kHz (from 320 to –420 ppm) is sufficiently wide to cover the chemical shift range for ^{29}Si nuclei in tetrahedral and octahedral sites. The spectrum was accumulated 1500 times with a recycle time of 2.5 s. Samples in an alumina sample holder were spun at the magic angle (54.74°) with respect to the external magnetic field. The spinning rate was 3500–4000 Hz. The chemical shift standard, Q_8M_8 , was used as a secondary standard whose chemical shift from TMS was set to 11.51 ppm.

A static (no sample spinning) ^{29}Si NMR was also employed to observe the chemical shift anisotropy, which could be almost removed by the MAS technique. The conditions for static ^{29}Si NMR measurements were the same as those in MAS NMR measurements except for the pulse width (5 μs).

^{27}Al NMR measurements were carried out with Bruker MSL-200 spectrometer operated at 52.148 MHz. The sweep width was 50 kHz (from 478 to –478 ppm), and an Al-free zirconia sample holder was used. To cut off the background signal from NMR probe head, a relatively long dead-time delay (400 μs) was used. The spectrum was accumulated 10 000 times with a repetition time interval of 0.1 s. External chemical shift standard of 1 M $\text{Al}(\text{NO}_3)_3$ solution was used.

Results

Typical ^{29}Si MAS NMR spectra (series 2b) are shown in Figure 2. The spectra were well reproduced by several Gaussian functions. However, the distinct peaks assigned Q_2 and Q_3 became ambiguous as aluminum ion was incorporated. The spectra of glasses of series 1 and 5 showed no more than a single peak with a relatively low S/N ratio at a high content of aluminum oxide. So the fitting by a single Gaussian peak was performed in these spectra. The derived chemical shift values are summarized in Table I. All the values of chemical shifts fall in ranges expected when the Si atom are in tetrahedral (not octahedral) environments.

The ^{27}Al MAS NMR measured as to the same glasses gave chemical shift values around 60 ppm, and no peak was found around 0 ppm (the shift of Al in six coordinated environments is 0–20 ppm). In the quadrupole nuclei ($I > 1/2$) such as ^{27}Al , the center of gravity of the observed NMR line shape shifts by the quadrupole interaction to higher field (more shielded) depending on the magnitude of the quadrupole interaction parameter (C_Q). The observed chemical shift in the present work (at 4.7 T) is estimated to be shifted about –10 ppm from the isotropic chemical shift when we consider $C_Q = 2.0$ MHz of the Na–Y zeolite.¹⁶ The estimated isotropic chemical shift (around 70 ppm) fall in the range of the shift of Al in four coordinated tetrahedral environments (55–80 ppm).

While an addition of Al_2O_3 to sodium silicate glasses (series 1) caused mild change in ^{29}Si chemical shifts, the substitution of

(19) Lowenstein, W. *Am. Mineral.* 1954, 39, 92.

(20) Maekawa, H.; Maekawa, T.; Kawamura, K.; Yokokawa, T. *J. Non-Cryst. Solids* 1991, 127, 53.

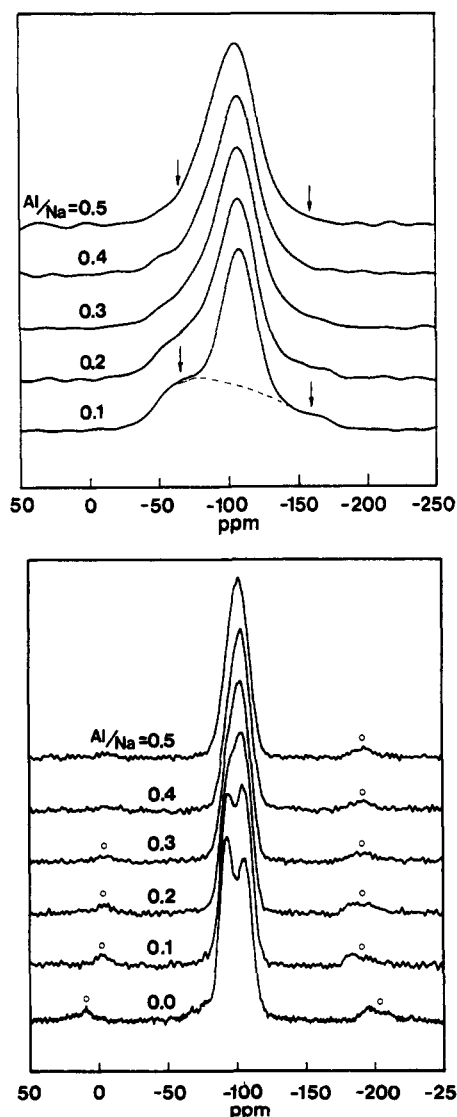


Figure 3. (Top) broad line and (bottom) MAS NMR spectra for series 3 glasses. Open circles shown in the bottom represent spinning sidebands.

neighboring Si atom by NaAl (series 5) caused a stronger shift to the lower field (less shielded). These trends are in agreement with the measurements for CaO–Al₂O₃–SiO₂ system.¹⁸ Furthermore, as the results of the series 2 glasses (Table IIa–c) clearly show, the effects of substitution of SiO₂ by NaAlO₂ upon the ²⁹Si chemical shifts are different for each coordination environment (Q_n's). The peak position of the more polymerized site (for example, the Q₃ site in series 2b glasses) is more affected by the addition of NaAlO₂ than that of the less polymerized site (Q₂).

Discussion

Chemical Shifts. The feature of ²⁹Si NMR line shapes is mainly characterized by the chemical shift anisotropy which had been observed in Q₃, Q₂, and Q₁ environments.^{21,22} In Figure 3 are shown the ²⁹Si broad-line and MAS NMR spectra for series 3 glasses. The broad-line NMR spectrum for glass of N_{Al} = 0.1 (Figure 3, top) consists of two peaks by Q₃ (showing chemical shift anisotropy; dashed line) and Q₄ site (single Gaussian). The substitution of Na atom by Al atom (Figure 3, top, N_{Al} = 0.2–0.5) caused the decrease of chemical shift anisotropic feature and increase of the broadening of Q₄ peak. We obtain a linear decrease of Q₃ site population with ([Na] – [Al])/[Si] ratios from the line-shape fitting for MAS NMR spectra of this glass (Figure 3, bottom, and Table II d). This suggests that the connection of

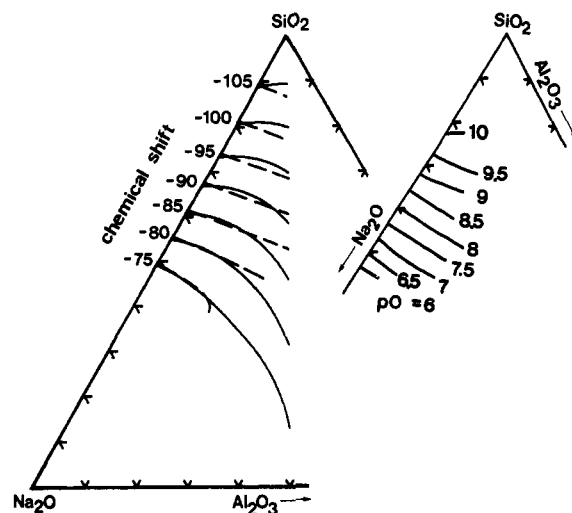


Figure 4. Left: ²⁹Si NMR isochemical shift lines as a function of the composition calculated by eq 2 assuming Lowenstein's rule is obeyed (solid) and not obeyed (broken). Right: Thermodynamic basicity derived from emf measurements.²²

the nonbridging oxygen is restricted only to Si atom, in agreement with the classical structural model.

In the following, a more detailed treatment for chemical shift analysis based on the structural model was tried. The overall chemical shifts of sodium aluminosilicate glasses could be represented as a function of N_{nbo} and N_{Al} by

$$\Delta(\text{ppm}) = N_{\text{nbo}}\Delta_{\text{Na}} + N_{\text{Al}}\Delta_{\text{NaAl}} + C_0 \quad (2)$$

where C₀ is the chemical shift value for pure silica glass referenced from TMS and Δ_{Na} and Δ_{NaAl} are the ²⁹Si chemical shifts induced on the central Si atom of a SiO₄ tetrahedron by each substitution of the next nearest neighbor (NNN) SiO₄ to Na (NBO formation) and NaAlO₄ (a Si–O–Al bond formation), respectively. In binary sodium silicate glasses, the chemical shifts do not depend linearly upon N_{nbo}, but the changes became gentle as alkali-metal cation contents increased. So the Δ_{Na} and Δ_{NaAl} will further depend on the bulk glass composition in the following way:

$$\Delta_{\text{Na}} = C_1 N_{\text{nbo}} + C_2 N_{\text{Al}} + C_3 \quad (3)$$

$$\Delta_{\text{NaAl}} = C_2 N_{\text{nbo}} + C_4 N_{\text{Al}} + C_5 \quad (4)$$

where Δ_{Na} and Δ_{NaAl} are assumed to be lowered by Na and/or NaAlO₄ that already exist on the NNN of the central Si atom and depend linearly on their numbers by the degree of C₁, C₂, and C₄. The coefficients C₀–C₅ were determined from the least-squares fit for 54 experimental values of weighted mean ²⁹Si chemical shifts in two cases when Lowenstein's rule was obeyed (i.e., N_{Al} = 4[Al]/[Si]) (C₀ = –110.0, C₁ = –3.6, C₂ = –1.7, C₃ = 24.2, C₄ = –0.8, and C₅ = 9.7) and was not obeyed (i.e., N_{Al} = 4[Al]/([Si] + [Al])) (C₀ = –111.0, C₁ = –3.5, C₂ = –2.8, C₃ = 24.6, C₄ = –1.3, and C₅ = 14.6) with standard deviations of 0.90 and 0.92, respectively. The induced ²⁹Si chemical shift of NNN substitution is almost twice as large for Na than NaAlO₄. The lines of isochemical shift calculated from the present experimental data with eqs 3 and 4 are shown in Figure 4, left. The isochemical shift lines change their slopes at the compositions near [Na]/[Al] = 1, and these changes are drastic in the SiO₂ poor region especially when Lowenstein's rule was not taken into consideration. The chemical shift value for CaAl₂SiO₆ glass¹⁷ was well reproduced by the latter postulate.

It has been shown that the ²⁹Si NMR chemical shifts have a potential parameter for the scale for basicity.²⁰ The thermodynamic basicities for this system (Figure 4, right),²³ which was defined by pO = –log (a_{Na₂O}) where a_{Na₂O} denotes the thermodynamic activity and determined from emf measurements, show close similarity with ²⁹Si isochemical shift lines.

(21) Stebbins, J. F. *Nature* 1987, 330, 465.

(22) Wilson, M. A. *NMR techniques and applications in geochemistry and soil chemistry*; Pergamon Press: Oxford, 1987; Chapter 5.

(23) Itoh, H.; Yokokawa, T. *Trans. J. I. M.* 1984, 25, 879.

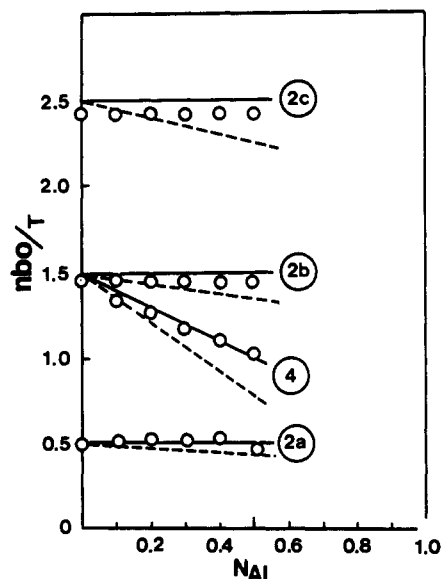


Figure 5. Numbers of nonbridging oxygen atoms per tetrahedral atom (Al + Si) obtained from NMR peak area analysis (open circle). The lines represent the calculated one on the assumption of the association of the nonbridging oxygen only with silicon atom (solid) and both silicon and aluminum (broken).

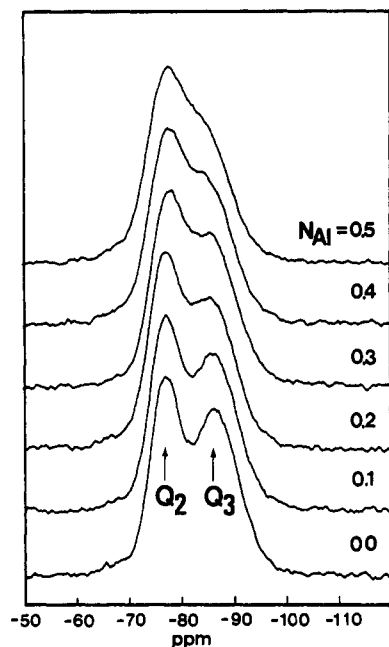


Figure 6. ^{29}Si MAS NMR spectra for series 2b glasses with different N_{Al} values.

Calculated Number of Nonbridging Oxygen Atoms. Figure 5 represents the relation between the number of nonbridging oxygen atoms per silicon atom and the added sodium aluminate (series 2–4). Here, solid lines are those calculated with the assumption that the excess sodium oxide modifies the Si–O–Si bond exclusively.

Alternatively if nonbridging oxygen atoms are assumed to be associated equally with both Si and Al atoms, the broken lines are obtained. Although the absolute values are somewhat smaller than the expected ones, the experimental values are better represented by the former postulate. The structural model is supported again.

Location of AlO_4 Tetrahedron. It is interesting where the AlO_4 tetrahedron is located in the silicate network. Figure 6 shows the ^{29}Si NMR line shapes for series 2b glasses. The main change occurs on the Q_3 peak. They were broadened and shifted to the lower field (less shielded) with an increase of N_{Al} . Figure 7 shows the changes of the chemical shifts for each peak in the glasses

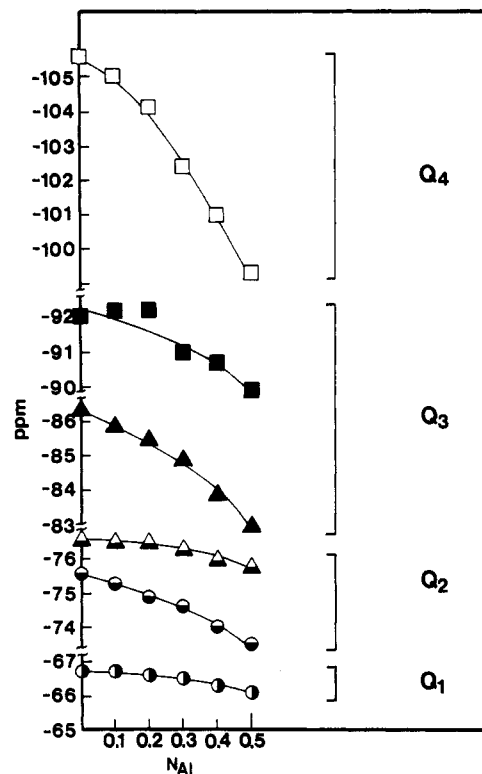


Figure 7. ^{29}Si chemical shift of structural units as functions of N_{Al} (\square , \blacksquare); series 2a ($1\text{Na}_2\text{O}\cdot 4\text{SiO}_2 + \text{NaAlO}_2$) (\triangle , \blacktriangle); series 2b ($3\text{Na}_2\text{O}\cdot 4\text{SiO}_2 + \text{NaAlO}_2$) and (\circ , \bullet); series 2c ($5\text{Na}_2\text{O}\cdot 4\text{SiO}_2 + \text{NaAlO}_2$) glasses.

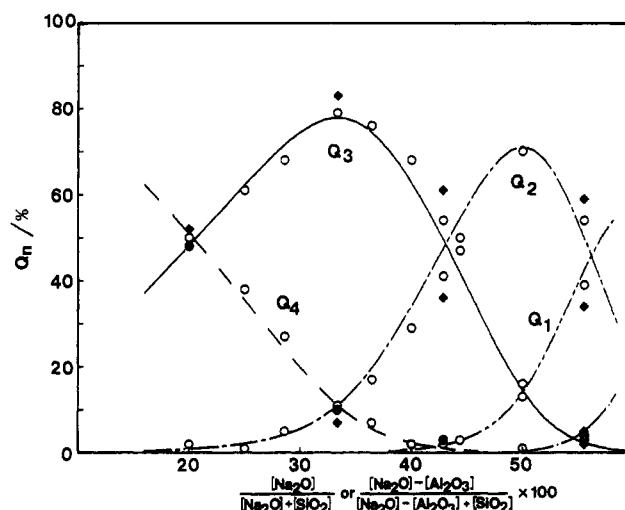


Figure 8. Q_n distribution as a function of contents of Na_2O : (\circ) for binary sodium silicate glass;²¹ (\bullet) present work at $N_{\text{Al}} = 0.5$.

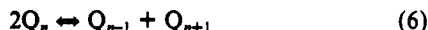
of series 2a–2c as a function of N_{Al} . The Si atoms in the most polymerized environment in the glass are most affected by the introduction of NaAlO_2 into the glass. For example, in the glasses of series 2c, the Q_2 peak shifts to lower field (less shielded) with an increase in the NaAlO_2 content. On the other hand, the Q_1 peak does not change so much. In this glass, the networks consist of mainly Q_2 and Q_1 species, and the following equilibria could be written in the presence of NaAlO_2 :



where $Q_2(1\text{Al})$ and $Q_1(1\text{Al})$ represent the silicon site with two and one bridging oxygen atoms in which one of them is connected to an aluminum atom, respectively. The present data suggest the equilibria of eq 5 type shift to the right side. Thus aluminum favors the more polymerized environments, i.e., the smaller number of nonbridging oxygen atoms. In terms of thermodynamic acid–base, Al_2O_3 is a stronger acid than SiO_2 and tends to be

associated with Na_2O to become NaAlO_2 , whereas NaAlO_2 is no more acidic than SiO_2 and additional Na_2O modifies not NaAlO_2 but SiO_2 .

Q_n Distribution. Basic oxides modify SiO_2 network depending upon their basicity or inversely upon the cationic power of the alkali cation (charge Z divided by ionic radius r). In addition to this, the resultant Q_n species are further affected by basicity in their distribution:



Thus, the stronger the cationic power of the alkali-metal cation, the more reaction 6 goes to the right.²⁰ The Q_n distribution for $N_{\text{Al}} = 0.5$ glasses derived from the present work is shown in Figure 8 together with the previous results of sodium silicate glasses. The Q_n distribution suggests that eq 6 shifts to the left with addition

of NaAlO_2 . This supports the opinion mentioned above that the NaAlO_2 acts as a base in sodium silicate glasses.

Conclusion

^{29}Si MAS NMR were investigated on sodium aluminosilicate glasses. The results indicate (1) that the number of nonbridging oxygen atoms could be determined by an excess amount of sodium ions over aluminum ions and in terms of thermodynamic acid-base, NaAlO_2 is no more acidic than SiO_2 and additional Na_2O modifies not NaAlO_2 but SiO_2 , although Al_2O_3 is more acidic than SiO_2 and is preferentially attacked by Na_2O to become NaAlO_2 , (2) that the aluminum ion favors the site in the rather polymerized part of silicate network, and (3) that introduction of Al_2O_3 induces the lower field shift (less shielding) of ^{29}Si NMR peak in addition to the chemical rearrangement reactions.

Infrared Spectroscopic Characterization of the Trimethylgallium-Arsine Adduct

Elizabeth A. Piocos and Bruce S. Ault*

Department of Chemistry, University of Cincinnati, Cincinnati, Ohio 45221 (Received: February 4, 1991; In Final Form: April 8, 1991)

The initial reaction product of the $(\text{CH}_3)_3\text{Ga}/\text{AsH}_3$ system has been studied by infrared spectroscopy. When these two reagents were codeposited into argon and nitrogen matrices, clear evidence of 1:1 complex formation was observed. Vibrational modes shifted 10–50 cm^{-1} in the complex relative to parent band positions. Band assignments were made by analogy to parent band positions and confirmed by deuterium labeling experiments. The spectra suggest a C_{3v} structure for the complex, with distinct distortion from planarity of the GaC_3 skeleton. Room temperature spectra in a static gas cell gave evidence for existence of the adduct at 295 K, either in the gas phase or condensed in the liquid phase on the windows of the gas cell.

Introduction

Metal-organic chemical vapor deposition (MOCVD) is widely used for the production of semiconductor thin films such as gallium arsenide and related III-V compounds.^{1–6} These films have a wide range of applications, particularly in the solar energy conversion and microelectronics fields. While these reactions are of great interest and importance, little is known about the details of the reaction mechanism, including the identity of potential intermediate species. The most common precursors for GaAs formation⁷ are $(\text{CH}_3)_3\text{Ga}$ and AsH_3 , with an overall reaction leading to GaAs and CH_4 . On the basis of the Lewis acid-base concepts,⁸ an initial adduct between $(\text{CH}_3)_3\text{Ga}$ and AsH_3 might be anticipated, yet its existence and role in MOCVD has been debated. Very recent ab initio calculations⁹ on the analogous $\text{H}_3\text{Ga}\cdot\text{AsH}_3$ system suggest that this adduct should be stable, and observable both in cryogenic matrices and in the gas phase.

The matrix isolation technique is ideally suited for the spectroscopic characterization of highly reactive and/or weakly bound chemical intermediates.^{10–12} Many classes of intermediates have been stabilized in this manner, including radicals, ions, hydrogen-bonded complexes, and molecular adducts. Recently, a study of the $(\text{CH}_3)_3\text{Ga}/\text{AsH}_3$ system was undertaken in this laboratory, and preliminary identification of this elusive adduct in argon matrices was reported.¹³ This study was subsequently extended to isotope labeling, thin film, and gas-phase experiments; the complete results are reported here.

Experimental Section

The matrix isolation and thin film experiments in the present study were all carried out on conventional matrix isolation equipment which has been described.^{14,15} $(\text{CH}_3)_3\text{Ga}$ (Alfa Products) and AsH_3 (Alphagaz) were introduced as gases into

the vacuum system and purified by freeze-thaw cycles at 77 K. AsD_3 was synthesized¹⁶ by the reaction of finely divided Zn_3As_2 with a 30% D_2SO_4 solution, followed by drying over CaCl_2 and purification by vacuum distillation. Argon and nitrogen were used without further purification as matrix gases.

Matrix samples were codeposited in either the twin-jet mode, where the two gas samples were sprayed simultaneously on the cold window from two separate nozzles, or in the merged-jet mode. In this latter approach, the two deposition lines were joined with an Ultratorr tee approximately 30 cm from the nozzle. The two gas samples then mixed during the flight time from the tee to the window, allowing for additional mixing time compared to the twin-jet mode, but without the static equilibration which occurs

(1) Moss, S. G.; Ledwith, A., Eds. *The Chemistry of the Semiconductor Industry*; Chapman and Hall: New York, 1987.

(2) Sherman, A. *Chemical Vapor Deposition for Microelectronics*; Noyes Data Corp.: Park Ridge, NJ, 1989.

(3) Hersee, S. D.; Duchemin, J. P. *Annu. Rev. Mater. Sci.* **1982**, *12*, 65.

(4) Sweibel, K. *Chem. Eng. News* **1986**, July 7, 34.

(5) Townsend, W. G.; Uddin, M. E. *Solid State Electron.* **1973**, *16*, 39.

(6) Larsen, C. A.; Li, S. H.; Buchan, N. I.; Stringfellow, G. B.; Brown, D. B. *J. Cryst. Growth* **1990**, *102*, 126.

(7) Manasevit, H. M. *Appl. Phys. Lett.* **1968**, *12*, 156.

(8) Jensen, W. B. *The Lewis Acid/Base Concepts; an Overview*; Wiley-Interscience: New York, 1980.

(9) Dobbs, K. D.; Trachtman, M.; Bock, C. W.; Cowley, A. H. *J. Phys. Chem.* **1990**, *94*, 5210.

(10) Whittle, E.; Dows, D. A.; Pimentel, G. C. *J. Chem. Phys.* **1954**, *22*, 1943.

(11) Craddock, S.; Hinchliffe, A. J. *Matrix Isolation*; Cambridge University Press: New York, 1975.

(12) Hallam, H. E., Ed. *Vibrational Spectroscopy of Trapped Species*; Wiley: New York, 1973.

(13) Piocos, E. A.; Ault, B. S. *J. Am. Chem. Soc.* **1989**, *111*, 8978.

(14) Ault, B. S. *J. Am. Chem. Soc.* **1978**, *100*, 2426.

(15) Ault, B. S. *Rev. Chem. Intermed.* **1988**, *9*, 233.

(16) Bauer, G. *Handbook of Preparative Inorganic Chemistry*; Academic Press: New York, 1963.

* Author to whom correspondence should be addressed.